

Hamilton-Jacobi equation with non-convex Hamiltonians in three dimensional level set simulations of the wet etching of silicon

BRANISLAV RADJENović¹, MARIJA RADMILOVIĆ-RADJENović²

¹Laboratory of Physics, Vinča Institute of Nuclear Sciences

P. O. Box 522, 11001 Belgrade

SERBIA

²Institute of Physics

Pregrevica 118, 11080 Belgrade

SERBIA

bradjeno@vin.bg.ac.yu

Abstract: - In this paper we have shown that profile evolution during anisotropic wet etching of silicon can be described by the non-convex Hamiltonian arising in the Hamilton-Jacobi equation for the level set function. Angular dependence of the silicon etching rate is determined on the basis of the silicon crystal symmetry properties.

Key-Words: - Hamilton-Jacobi equation, non-convex Hamiltonian, level set method, wet etching, silicon, MEMS, profile evolution

1 Introduction

Level set method, introduced by Osher and Sethian [1], is a powerful technique for analyzing and computing moving fronts in a variety of different settings. The level sets are used in image processing, computer vision, computational fluid dynamics, material science, and many other fields. Detailed exposition of the theoretical and numerical aspects of the method, and applications to different areas can be found in books [1] and [2].

During last several years several variants of level set methods have been developed with application to microelectronic devices fabrication problems. The profile surface evolution in etching, deposition and lithography development is a significant challenge for implementation of numerical methods in front tracking. The level set methods for evolving interfaces are specially designed for profiles which can develop sharp corners, change of topology and undergo orders of magnitude changes in speed. They are based on Hamilton–Jacobi type equation for the level set function using techniques developed for solving hyperbolic partial differential equations. In this paper we describe shortly the level set method as well as sparse field method for solving the level set equations. The sparse-field method itself, developed by Whitaker [3], and broadly used in image processing community, is an alternative to the usual combination of narrow band and fast marching

procedures for the computationally effective solving of the level set equations. After that we analyze the case of non-convex Hamiltonians and its application in the simulations of the etching profile evolution during anisotropic wet etching of silicon with KOH etchant in more details. This type of problem is of special interest in studying the evolution of the profile surface during the etching process, especially if we treat it as an interface controlled problem.

2 Level Set Method for Non-convex Hamiltonians

The basic idea behind the level set method is to represent the surface in question at a certain time t as the zero level set (with respect to the space variables) of a certain function $\varphi(t, \mathbf{x})$, the so called level set function. The initial surface is given by $\{\mathbf{x} \mid \varphi(0, \mathbf{x}) = 0\}$. The evolution of the surface in time is caused by “forces” or fluxes of particles reaching the surface in the case of the etching process. The velocity of the point on the surface normal to the surface will be denoted by $V(t, \mathbf{x})$, and is called velocity function. For the points on the surface this function is determined by physical models of the ongoing processes. The velocity function generally depends on the time and space variables and we assume that it is defined on the whole simulation domain. At a later time $t > 0$, the surface is as well the zero level set of the function $\varphi(t, \mathbf{x})$, namely it can be defined as a set

of points $\{\mathbf{x} \in \mathfrak{R}^n \mid \varphi(t, \mathbf{x}) = 0\}$. This leads to the level set equation

$$\frac{\partial \varphi}{\partial t} + V(t, \mathbf{x}) |\nabla \varphi| = 0, \quad (1)$$

in the unknown function $\varphi(t, \mathbf{x})$, where $\varphi(0, \mathbf{x}) = 0$ determines the initial surface. Having solved this equation the zero level set of the solution is the sought surface at all later times. Actually, this equation relates the time change to the gradient via the velocity function. In the numerical implementation the level set function is represented by its values on grid nodes, and the current surface must be extracted from this grid. In order to apply the level set method a suitable initial function $\varphi(0, \mathbf{x})$ has to be defined first. The natural choice for the initialization is the signed distance function of a point from the given surface. As already stated, the values of the velocity function are determined by the physical models.

The equation (1) can be rewritten in Hamilton-Jacobi form

$$\frac{\partial \varphi}{\partial t} + H(\nabla \varphi(t, \mathbf{x})) = 0, \quad (2)$$

where Hamiltonian is given by

$$H = V(t, \mathbf{x}) |\nabla \varphi(t, \mathbf{x})| \quad (3)$$

(in this context the term ‘‘Hamiltonian’’ denotes a Hamiltonian function, not an operator). A detailed exposition about the Hamilton–Jacobi equation, the existence and uniqueness of its solution (especially about its viscosity solutions), can be found in [4]. We say that such a Hamiltonian is convex (in \mathfrak{R}^n) if the following condition is fulfilled

$$\frac{\partial^2 H}{\partial \varphi_{x_i} \partial \varphi_{x_j}} \geq 0, \quad (4)$$

where φ_{x_i} is a partial derivative of $\varphi(t, \mathbf{x})$ with respect of x_i . If the surface velocity $V(t, \mathbf{x})$ does not depend on the level set function $\varphi(t, \mathbf{x})$ itself, this condition is usually satisfied. In that case, we can say that the problem is of free boundary type. In that case the spatial derivatives of φ can be approximated using the Engquist–Osher upwind finite difference scheme, or by ENO (higher-order essentially non-oscillatory) and WENO (weighted essentially non-oscillatory) discretization schemes, that requires the values of this function at the all grid points considered. The resulting semi-discrete equations can be solved using explicit Euler method, or more precisely by TVD (total-variation diminishing) Runge-Kutta time integration procedure (see ref. [2] for the details).

Several approaches for solving level set equations exist which increase accuracy while decreasing computational effort. They are all based on using some sort of adaptive schemes. The most important are narrow band level set method [1], widely used in etching process modeling tools, and recently developed sparse-field method [3], implemented in medical image processing ITK library [5]. The sparse-field method use an approximation to the distance function that makes it feasible to recompute the neighborhood of the zero level set at each time step. In that way, it takes the narrow band strategy to the extreme. As a result, the number of computations increases with the size of the surface, rather than with the resolution of the grid.

The upwind finite difference scheme cannot be used in the case of non-convex Hamiltonians. The simplest scheme that can be applied in these cases is the Lax–Friedrichs, one which relies on the central difference approximation to the numerical flux function, and preserves monotonicity through a second-order linear smoothing term [2]:

$$\begin{aligned} \varphi_{ijk}^{n+1} = \varphi_{ijk}^n - \Delta t [H & \left(\frac{D_{ijk}^{-x} + D_{ijk}^{+x}}{2}, \frac{D_{ijk}^{-y} + D_{ijk}^{+y}}{2}, \frac{D_{ijk}^{-z} + D_{ijk}^{+z}}{2} \right) \\ & - \frac{1}{2} \alpha_x (D_{ijk}^{+x} - D_{ijk}^{-x}) - \frac{1}{2} \alpha_y (D_{ijk}^{+y} - D_{ijk}^{-y}) - \frac{1}{2} \alpha_z (D_{ijk}^{+z} - D_{ijk}^{-z})] \end{aligned} \quad (5)$$

where $D_{ijk}^{+x(y,z)}$ and $D_{ijk}^{-x(y,z)}$ are usual forward and backward differences:

$$\begin{aligned} D_{ijk}^{+x} &= \frac{\varphi_{i+1,j,k}^n - \varphi_{i,j,k}^n}{\Delta x}, & D_{ijk}^{-x} &= \frac{\varphi_{i,j,k}^n - \varphi_{i-1,j,k}^n}{\Delta x} \\ D_{ijk}^{+y} &= \frac{\varphi_{i,j+1,k}^n - \varphi_{i,j,k}^n}{\Delta y}, & D_{ijk}^{-y} &= \frac{\varphi_{i,j,k}^n - \varphi_{i,j-1,k}^n}{\Delta y}, \\ D_{ijk}^{+z} &= \frac{\varphi_{i,j,k+1}^n - \varphi_{i,j,k}^n}{\Delta z}, & D_{ijk}^{-z} &= \frac{\varphi_{i,j,k}^n - \varphi_{i,j,k-1}^n}{\Delta z} \end{aligned} \quad (6)$$

and $\alpha_x(\alpha_y, \alpha_z)$ is a bound on the partial derivative of the Hamiltonian with respect to the first (second, third) argument:

$$\alpha_x = \max \left| \frac{\partial H}{\partial \varphi_x} \right|, \quad \alpha_y = \max \left| \frac{\partial H}{\partial \varphi_y} \right|, \quad \alpha_z = \max \left| \frac{\partial H}{\partial \varphi_z} \right|. \quad (7)$$

The terms on the second row of the equation (5) are the smoothing terms. In general, these terms need not be calculated exactly. Overestimated values will produce non-realistic smoothing of the sharp corners in the implicit surfaces. Too little smoothing usually leads to numerical instabilities in calculations. In [6] we have shown show that it is possible to use the Lax–Friedrichs scheme in conjunction with the

sparse field method, and to preserve sharp interfaces and corners by optimizing the amount of smoothing in it.

2 Anisotropic Wet Etching of Silicon

Anisotropic wet chemical etching remains the most widely used processing technique in silicon MEMS technology [7]. Very complicated three-dimensional structures can be formed by this technique. KOH is the most common and the most important etchant, and we shall use the numerical values characterizing it here. In order to simulate the time evolution of three dimensional etching profiles it is essential that exact etch rates in all directions are known. In this paper we shall use etching rate model developed by Hubbard [8]. The etching rates for only a few principal axes are known, but they can be used to determine rate value in an arbitrary direction \mathbf{N} (N_x, N_y, N_z) by an interpolation procedure. It is supposed that N_x, N_y and N_z axes are aligned with [100], [010] and [001] crystal directions, respectively. In actual calculations we made use of measured etching rates in [100], [110] and [111] crystal directions, for 30% KOH concentration at 70°C from ref. [9] ($R_{100} = 0.797\mu\text{m}/\text{min}$; $R_{110} = 1.455\mu\text{m}/\text{min}$; $R_{111} = 0.005\mu\text{m}/\text{min}$).

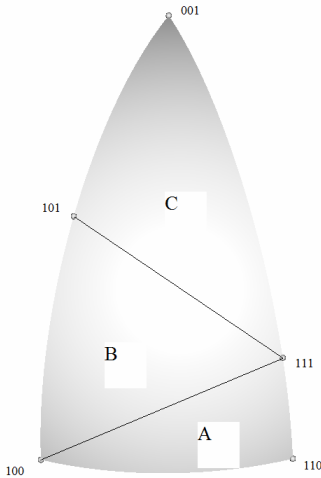


Fig. 1: Etching rate model regions

The point group of silicon's symmetry $m3m$ (subgroup of $Fd3m$ space group) contains 48 elements. Since it is not possible to assemble angular section using 3 principal directions with which the whole space can be covered by the symmetry operations, only 16 out of 48 symmetry elements can be used for that purpose. As a result, it is necessary to look only at 1/16th of the full angular extent, that is actually the union of three sections defined by the principal vectors A[100, 111, 110], B[100, 111, 101] and C[001, 111, 101], which is shown in Fig. 1.

The etching rate R in an arbitrary direction defined by vector \mathbf{N} is given by an interpolation relation [8]:

$$R(\mathbf{N}) = \begin{cases} \left[R_{100}(N_x - N_y) + R_{110}(N_y - N_z) + R_{111}N_z \right] / N_x; & \mathbf{N} \in A \\ \left[R_{100}(N_x - N_z) + R_{110}(N_z - N_y) + R_{111}N_y \right] / N_x; & \mathbf{N} \in B \\ \left[R_{100}(N_z - N_x) + R_{110}(N_x - N_y) + R_{111}N_y \right] / N_z; & \mathbf{N} \in C \end{cases} \quad (8)$$

Etching rate angular dependence can be obtained by introducing spherical angular coordinates ϕ and θ instead of Cartesian (N_x, N_y, N_z):

$$N_x = \sin \theta \cos \phi; N_y = \sin \theta \sin \phi; N_z = \cos \theta \quad (9)$$

Substituting (9) in (8) we get desired angular dependence of the etching rate $R(\theta, \phi)$, which is shown in Fig. 2:

$$R(\theta, \phi) = \begin{cases} R_{100} - (R_{110} - R_{111}) \cot \theta / \cos \phi + (R_{110} - R_{100}) \tan \phi; & (\theta, \phi) \in A \\ R_{100} + (R_{110} - R_{100}) \cot \theta / \cos \phi + (R_{111} - R_{110}) \tan \phi; & (\theta, \phi) \in B \\ R_{100} + [(R_{110} - R_{100}) \cos \phi + (R_{111} - R_{100}) \sin \phi] \tan \theta; & (\theta, \phi) \in C \end{cases} \quad (10)$$

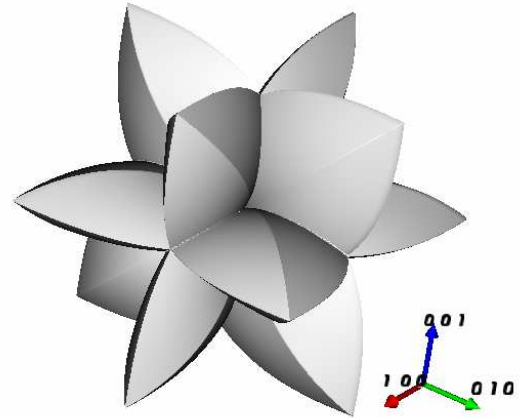


Fig. 2: Etching rate angular dependence

The anisotropic etching rate $R(\mathbf{N})$ is actual velocity function $V(t, \mathbf{x})$ in our profile evolution model. So, by substituting (8) in (3) and (2), the Hamiltonian function is obtained:

$$H(\nabla\phi) = \begin{cases} |\nabla\phi| \left[R_{100}\phi_x + (R_{110} - R_{100})\phi_y + (R_{111} - R_{110})\phi_z \right] / \phi_x; & \nabla\phi \in A \\ |\nabla\phi| \left[R_{100}\phi_x + (R_{111} - R_{110})\phi_y + (R_{100} + R_{110})\phi_z \right] / \phi_x; & \nabla\phi \in B \\ |\nabla\phi| \left[(R_{110} - R_{100})\phi_x + (R_{111} - R_{110})\phi_y + R_{100}\phi_z \right] / \phi_z; & \nabla\phi \in C \end{cases} \quad (11)$$

Non-convexity of this Hamiltonian can be checked using relation (4) directly, which is a non-trivial task, but it is no necessary since it follows indirectly from the shape of the rate function, shown in Fig. 2.

3 Simulation Results

The results shown in this section are obtained by solving equation (2) with Hamiltonian defined by (11) on $256 \times 256 \times 256$ Cartesian grid. The actual shapes of the initial surfaces are described using simple geometrical abstractions. In the beginning of the calculations this descriptions are transformed into the initial level set functions using the fast marching method. Our implementation is based on ITK library. The classes describing the level set function and the level set filter are reimplemented according to the procedures for treating non-convex Hamiltonians described in the previous section.

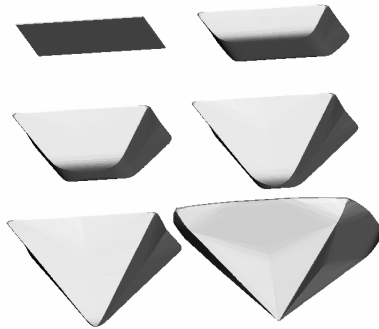


Fig. 3: Wet etching through a rectangular mask

The first example is etching through a square open window in the $\{100\}$ silicon plane with edges aligned to the $\langle 110 \rangle$ directions. The time evolution of the etched profile is shown in Fig. 3. Formation of the cavity consisting of only $\{111\}$ plane is reproduced correctly.

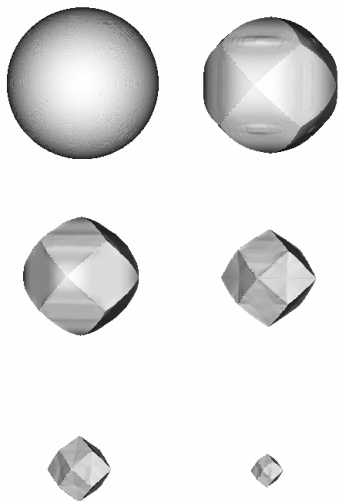


Fig. 4: Wet etching of silicon ball

In order to demonstrate the strength of the method we have chosen to simulate etching of the silicon ball in KOH etchant also. The initial spherical surface contains all possible velocity directions, so it

is expected that the anisotropy of the etching process will produce the most dramatic changes of the initial shape. This shape is used in the experimental setup for measuring etching rates anisotropy [10], also.

In Fig. 4 the changes of the initial spherical shape at five equidistant reduced time moments are shown. The influence of the etching rate anisotropy is clearly demonstrated. During the etching process the initial sphere collapses anisotropically. The etching rate is the smallest in the $[111]$ direction family and it corresponds to the peaks of the current shape, while the high rate directions $[110]$ are related to its depths.

4 Conclusion

In this paper we have presented an application of the sparse field method for solving Hamilton-Jacobi equation with non-convex Hamiltonian in the 3D simulations of the profile surface evolution during anisotropic etching of silicon. The obtained results show that sparse field level set method can be used as an effective tool for wet etching process modeling.

References:

- [1] J. Sethian, *Level Set Methods and Fast marching Methods: Evolving Interfaces in Computational Geometry, Fluid Mechanics, Computer Vision and Materials Sciences*, Cambridge University Press, Cambridge, UK, 1998.
- [2] S. Osher and R. Fedkiw, *Level Set Method and Dynamic Implicit Surfaces*, Springer-Verlag, New York, NY, 2003.
- [3] R. Whitaker, *The International Journal of Computer Vision*, Vol. 29, No. 3, 1998, pp 203-231
- [4] L. Evans, *Partial Differential Equations*, American Mathematical Society, Providence, RI, 1998.
- [5] NLM Insight Segmentation and Registration Toolkit, <http://www.itk.org>
- [6] B. Radjenović, J. K. Lee and M. Radmilović-Radjenić, *Computer Physics Communications* Vol. 174, 2006, pp. 127-132
- [7] M. Elwenspoek and H. V. Jansen, *Silicon Micromachining*, Cambridge University Press, Cambridge, UK, 1998.
- [8] T. J. Hubbard, "MEMS Design - Geometry of silicon micromachining", Ph.D. Thesis, California Institute of Technology, 1994. <http://etid.caltech.edu/etid/available/etid-09162005-134646>
- [9] K. Sato et al., *Sensors and Actuators A* 64, 1988, pp. 87-93
- [10] M. Shikida et al., *Sensors and Actuators A* 80, 200, pp. 179-188